5-1-2022

Topology optimization of an air-cooled heat sink for transient heat dissipation using a homogenization approach

A. Banthiya

S. Ozguc

L. Pan

Justin A. Weibel
jaweibel@purdue.edu

2022 21st IEEE Intersociety Conference on Thermal and Thermomechanical Phenomena in Electronic Systems (iTherm) | 978-1-6654-8503-6/22/$31.00 ©2022 IEEE | DOI: 10.1109/iTherm54085.2022.9899571

Topology Optimization of an Air-Cooled Heat Sink for Transient Heat Dissipation using a Homogenization Approach

Abhijeet Banthiya, Serdar Ozguc, Liang Pan, Justin A. Weibel*
School of Mechanical Engineering, Purdue University
West Lafayette, IN 47906, USA
Email*: jaweibel@purdue.edu

***Abstract* — A homogenization approach to topology optimization is utilized to optimize the thermal performance of air-cooled heat sinks. Under the homogenization approach, partial densities are physically represented as square air ducts of varying sizes concentric to the grid cell. This formulation allows the calculation of local heat transfer coefficients using correlations for flow inside a duct. Because many electronics applications require transient thermal management solutions due to time-varying or periodic workloads, a subroutine is discussed to characterize and improve the transient performance indicators of heat sinks using a steady optimization toolbox. This subroutine aims to improve the transient thermal performance of a heat sink by imposing a solid region over the heat input of the optimization domain. This increases the thermal capacitance of the heat sink to address transient spikes in heat input. Heat sinks with increasingly thick solid regions are optimized under a steady average heat load, and then the thermal performance of these optimized designs is evaluated in response to a transient heat load profile. The heat sink thermal performance is evaluated using thermal resistance for the steady heat load and peak and time-averaged maximum domain temperatures for a pulsed periodic heat load. It was observed that the time-averaged maximum domain temperature is directly related to the optimized thermal resistance under a steady heat load boundary condition. There exists an optimal solid region thickness at which the transient performance is most improved in terms of peak or time-averaged maximum domain temperatures. The work demonstrates an approach for heat sink topology optimization for managing thermal fluctuations under a periodic heat load.**

Keywords* — *topology optimization, transient, additive manufacturing, heat sink, thermal management

NOMENCLATURE

a	Square duct size, m
c_P	specific heat capacity, J/kg-K
h	Effective heat transfer coefficient, W/m^2-K
k	Effective thermal conductivity, W/m-K
l	Square grid cell size, m
l_w	Solid wall thickness over heat input, m
$\dot{m}$	Air mass flow rate, kg/s
M	Solid mass fraction
M_{max}	User-defined max allowed solid mass fraction
N	Total number of grid cells
q''	Cell heat flux, W/m^2
Q_{in}	Net heat input, W
R	Pseudo thermal resistance, K/W
R_{scale}	Thermal resistance scaling factor, K/W
$T_{f,in}$	Air inlet temperature, K
ΔT_f	Air inlet to outlet temperature rise, K
T_{max}	Maximum domain temperature, K
T_s	Average temperature of a cell, K
$\Delta T_{s,f}$	Average cell to air outlet temperature difference, K
max(T_{max})	Peak transient maximum temperature, K
avg(T_{max})	Time-averaged maximum temperature, K
Δz	depth, m

Greek symbols

ε_i	Design variable (cell porosity)
α	Penalization factor

I. INTRODUCTION

The increasing demand for computing capability coupled with trends toward more compact products has led to increased power densities in electronics systems [1,2]. The reliability of many electronic devices reduces with increasing temperature, and prolonged operation at high temperatures can lead to premature failure [3]. Therefore, heat dissipated by active electronic components needs to be effectively removed from the system with minimal temperature rise in the device.

Traditionally, thermal management of many electronic systems is handled by active or passive air cooling [4]. Passive aircooling relies on the density difference between the surface and colder surroundings to drive the airflow that removes heat from the system. Although passive systems are favorable for their simplicity when the cooling performance is sufficient, active air cooling using fans or blowers is often required to enhance the convective heat transfer coefficient. There has been some shift towards liquid cooling solutions that can handle higher power densities [5,6], largely owing to the higher thermal conductivity and heat capacity of liquids than air [7]. However, most standalone electronic systems still rely on air cooling, often in conjunction with passive heat spreaders such as heat pipes and vapor chambers [8]. As these systems continue to provide higher computational performance and functionalities to the user, there is a need for improved thermal management solutions that utilize air cooling.

Additive manufacturing (AM) allows controlled fabrication of complex geometries, offering the design freedom to enhance heat sink performance. With the advancements in powder-bed AM technologies, high-thermal-performance parts can be manufactured using high conductivity metals, with examples including heat sinks [9], microchannel heat exchangers [10], and vapor chambers [11]. To fully leverage the design freedom brought by AM, many recent studies have utilized formal design optimization methods. Topology optimization is one method used in a wide range of applications [12,13] that optimizes material distribution within a numerically discretized design space to minimize a user-defined objective function. The method has been used for thermal management components, such as in the topology optimization of a confined jet impingement heat sink by Dede et al. [14], which was additively manufactured and experimentally shown to have a higher coefficient of performance than benchmark heat sink geometries manufactured using conventional methods.

Topology optimization can be implemented in numerous algorithms [15], which all typically discretize the design space into small cells and optimize a design variable within each cell to control the material distribution. The most common method that has been used in the design of thermal management components has been a 'penalized' approach. Under this penalized approach, the material distribution is represented by a cell porosity design variable which can vary between 0 (solid phase) and 1 (fluid/void phase) in the design space. The partial porosities between the 0 and 1 extremes hold no physical meaning; therefore, the algorithm uses a penalization algorithm that increasingly penalizes the inclusion of such partial porosities, such that the final design comprises cells that are strictly 0 or 1. Ozguc et al. [16] developed a novel 'homogenization' approach to topology optimization wherein the partial porosities are physically represented by a microstructure having known properties as a function of the porosity. Advantages of this homogenization approach include: i) the ability to resolve sub-resolution features to significantly reduce computational expense; ii) intrinsically manufacturable designs due to the physical definition of partial porosities; iii) much fewer user-specified algorithmic inputs; (iv) a relaxed homogenization approach is more likely to reach near-optimal performance compared to restrictive penalized approaches; and (v) better representation of the physics throughout the optimization iterations as partial porosity material properties can be expressed with known analytical functions.

Topology optimization approaches are often limited to steady state analyses with constant heat loads and uniform heat transfer coefficients, despite various applications requiring the thermal management of transient heat pulses [17,18]. Temporal temperature oscillations can lead to failure of the electronic systems through fatigue [19]. Systems prone to such oscillation are often overdesigned with a significant safety factor to keep the peak transient temperatures well below critical limits [17], leading to lower efficiency and larger components. Despite the proven ability of topology optimization to design high-performing heat sinks that outperform their conventional counterparts, previous studies have not focused on managing the transient heat loads using topology optimization. A recent study by Wu et al. [20] proposed a new topology optimization method for the design of structures under transient heat conduction. They conclude that the optimized topology is highly dependent on the duration and form of the transient heat input. To date, there is no theoretical framework for topology optimization under transient convective heat transfer, which would pose an extreme computational challenge if attempting a transient solution to the governing conservation equations. An alternative approach is to use the extensive toolbox of steady topology optimization approaches, combined with intuition-based subroutines, to design parts intended for transient heat loads.

In this study, a steady topology optimization algorithm is first formulated to design a high-performance air-cooled heat sink. A homogenization approach is formulated that uses square air ducts of varying sizes to define the partial cell porosity. A key advantage of using the homogenization approach, with this representation for the porosity, is that a channel-size-dependent heat transfer coefficient can be locally calculated for each cell using correlations for flow inside a duct, without requiring simulation of the convection. In the formulation, sensible heating of airflow through the air ducts is also considered. The model optimizes individual cell porosity to minimize the peak temperature in the domain under a steady heat input. The thermal response of the steady-state optimized design to a periodic heat load is subsequently studied using transient numerical simulations. The second part of the paper discusses an intuition-based methodology to improve the transient response of steady-state optimized heat sink designs in response to a periodic pulsed heat load.

II. Methodology

A. Steady topology optimization of an air-cooled heat sink

In the design of an air-cooled heat sink, thermal resistance between the heater and the inlet coolant temperature is used to define the performance. Hence, an objective function to be minimized is formulated based on a measure of thermal resistance:

$$f_{obj}(\varepsilon_i) = \frac{R(\varepsilon_i)}{R_{scale}} + \alpha \left[\max\left(0,\ \frac{M(\varepsilon_i)}{M_{max}} - 1\right)\right]^2 \qquad (1)$$

where $0 \le \varepsilon_i \le 1,\ 0 \le M_{max} \le 1$

The form of this objective function is further explained in detail in the ensuing discussion.

For this study, maintaining the heat sink mass below a specified limit is also posed within the objective using an exterior penalty method. Namely, a positive value is added to the cost function when the constraint is violated, i.e., when the solid mass fraction of the design is higher than the specified limit. The optimizer then tries to reduce this added value at the expense of increased thermal resistance. The relative importance of the mass constraint over thermal resistance can be controlled using the penalization factor α. A higher penalization factor implies a stricter constraint. The penalty

function is squared to make the combined objective function differentiable.

The heat sink design space is discretized into small square cells, as shown in Fig. 1. Each cell is assigned a porosity ε_i, the design variable, which can vary between 0 and 1. The thermal resistance, $R(\varepsilon_i)$, and the total solid mass fraction, $M(\varepsilon_i)$, of the heat sink are dependent on the set of design variables ε_i. A constant scaling factor, R_{scale}, is used so that the ratio R/R_{scale} appearing in the objective function is of the same order as the value obtained from the mass penalization term. A user-defined maximum allowed solid mass fraction M_{max} of the heat sink has a value specified between 0 and 1.

Following a homogenization approach, partial porosities at each cell define a physical local geometry and transport properties. Each square cell is assumed to be a conducting solid containing a concentric square hole, or duct, through which there is convection to airflow, as shown in Fig. 1. The size of this air duct is defined from the cell porosity as

$$\varepsilon_i = \frac{a^2}{l^2} \tag{2}$$

where a is the side length of the square air duct, and l is the side length of the square cell. The topology optimization algorithm thereby optimizes the size of the duct by varying the cell porosity.

As heat is transferred from the solid mass in the cell to the air inside the duct through convection, the air heats up. Energy conservation equations for solid and fluid mediums (with local thermal non-equilibrium) are solved for the temperature distribution in the heat sink, respectively given by

$$-k(\varepsilon_i)\nabla T_s - h(\varepsilon_i)\Delta T_{s,f} = -\frac{q''}{\Delta z} \tag{3}$$

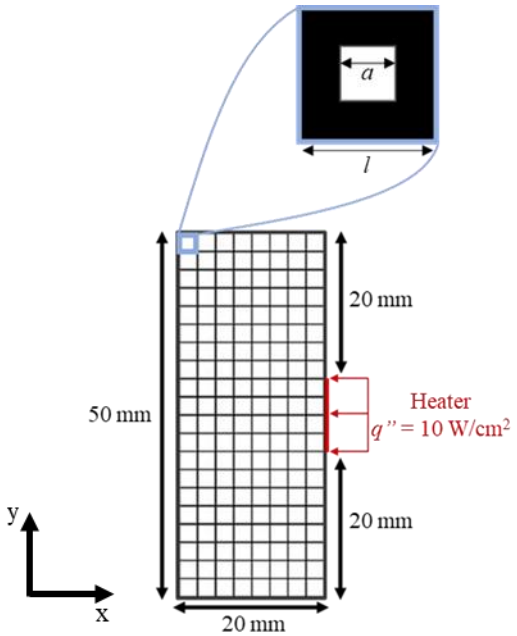

Fig. 1. Discretized design domain with dimensions, heater boundary condition, and representative domain cell used for steady topology optimization.

$$\dot{m}c_P\Delta T_f = h(\varepsilon_i)\Delta T_{s,f} \tag{4}$$

In the governing energy equations, $k(\varepsilon_i)$ is the cell's effective thermal conductivity. A polynomial function for the effective cell thermal conductivity versus porosity was developed by separately performing numerical simulations of heat conduction through the square cells at many different porosities. The air flows into the plane (normal to the x and y coordinates shown in Fig.1), through the air ducts in the cells. The heat transfer coefficient at the solid-fluid interface, $h(\varepsilon_i)$, a function of duct size and flow rate, is calculated using laminar and turbulent internal flow correlations. The maximum air temperature at the end of the duct outlet is used to calculate convective heat transfer from the cell; hence, $\Delta T_{s,f}$ represents the difference between the average local solid cell temperature T_s and air temperature at the duct outlet. The temperature rise from the duct inlet to outlet, ΔT_f, accounts for the sensible heating of air. A constant pressure drop boundary condition is assumed for calculating the flow through the duct. Boundary cells at the heater have a non-zero value of q'' to apply the heat input into the domain, where Δz is the depth of the heat sink in the third dimension. The governing differential equations are discretized using the finite volume method in two dimensions. The 2D discretized governing equations are solved using first-order derivatives in MATLAB.

As the model is evaluated during the optimization process, the calculated thermal resistance of the heat sink is defined in the following pseudo-functional form.

$$\mathrm{R}(\varepsilon_i) = \frac{1}{Q_{in}}\left[\frac{\sum (T_s - T_{f,in})^{\mathrm{m}}}{\mathrm{N}}\right]^{\frac{1}{\mathrm{m}}} \tag{5}$$

This pseudo thermal resistance is used instead of a definition based on the local maximum temperature of the domain to prevent an ill-posed objective function in the case where the cell location with maximum temperature moves with every iteration. In the pseudo thermal resistance, the difference between the cell temperature and inlet air temperature is raised to the exponent m and averaged over the design space. A higher value of m implies more weight is placed on the cells with higher temperatures. A large value of m = 10 is used in this study to prioritize the reduction of the maximum temperature within the domain. Solid mass fraction is defined using the cell porosities as

$$\mathrm{M}(\varepsilon_i) = \frac{\sum (1 - \varepsilon_i)}{\mathrm{N}} \tag{6}$$

where the value of $1 - \varepsilon_i$ defines the solid fraction of the cell, which is then averaged over the entire domain.

A sequential linear programming (SLP) method is utilized in this study for topology optimization. SLP solves a first-order approximating subproblem at each design iteration by linearizing the objective function and constraints. The sensitives (objective function gradients with respect to porosities) are calculated using the gradient information obtained from solving the adjoint problem using the adjoint state method [21]. The sensitivities are then filtered using a

filtering scheme developed by Sigmund [22] to avoid checkerboard patterning in the design. The resulting sensitivities are then utilized to update the design domain porosities. The optimization is run till convergence when the design stops changing with further iteration.

B. Transient performance of steady-state optimized heat sink

The designs obtained from steady topology optimization are characterized for their transient performance under a pulsed periodic heat load using transient numerical simulations in ANSYS Fluent with a fixed time step size of 0.1 s. The transient heat load case consists of a single heat input pulse held for a certain duty cycle, with zero heat input otherwise. The heat input boundary condition utilized for the steady optimization is the time-averaged value of the transient heat load. For characterizing the transient performance, the temperature distribution in the heat sink is first allowed to stabilize at the time-periodic response. After achieving this time-periodic solution, the maximum temperature T_{max} in the domain over time is tracked. The heat sink design is then characterized based on two different metrics: i) the peak of the maximum domain temperature, denoted as max(T_{max}), and ii) the average of the maximum domain temperature over a period, denoted as avg(T_{max}). The peak of the maximum domain temperature is always achieved at the end of the pulse during a cycle.

To reduce the peak temperature during a short transient heat input pulse, the thermal capacitance of the heat sink near the heat source needs to be increased [17]. This is because, at the initial times after the pulse, conduction is the predominant mode by which heat is initially dissipated from the heat source. Only at later times is there an increase in the temperature difference between the coolant and the convective solid-fluid surface, consequently increasing the contribution from convection. Conversely, this added thermal capacitance typically imposes a higher conduction resistance between the heat source and the convection surface (or a reduction in the available convective surface area), from which all heat must eventually be removed before the next pulse, increasing the average heat source temperature over time. With this understanding, an intuition-based approach is proposed to manage the peak temperature by balancing this tradeoff, wherein a solid wall of increasing thickness l_w is imposed in the domain over top of the heater, as shown in Fig. 2. This is implemented by forcing the porosities in these cells to always be equal to 0 (solid phase) during the optimization iterations. Each of these domains are optimized using the steady topology optimization algorithm, followed by performance characterization using the transient numerical simulations, to determine which provides the best transient performance metrics in the end.

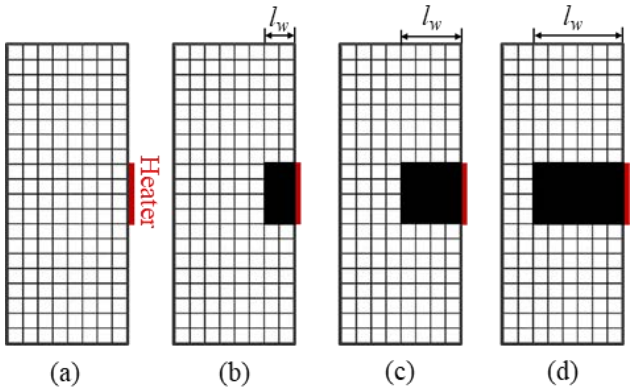

Fig. 2. Optimization design domains with an increasing wall thickness over top of the heater, where l_w is (a) 0 mm, (b) 5 mm, (c) 10 mm, and (d) 15 mm.

III. RESULTS

A 20 × 50 mm^2 design domain (Fig. 1) is discretized into square cells of side length 2.5 mm. A cell size of 2.5 mm was chosen after testing cases with different cell sizes (from 10 mm down

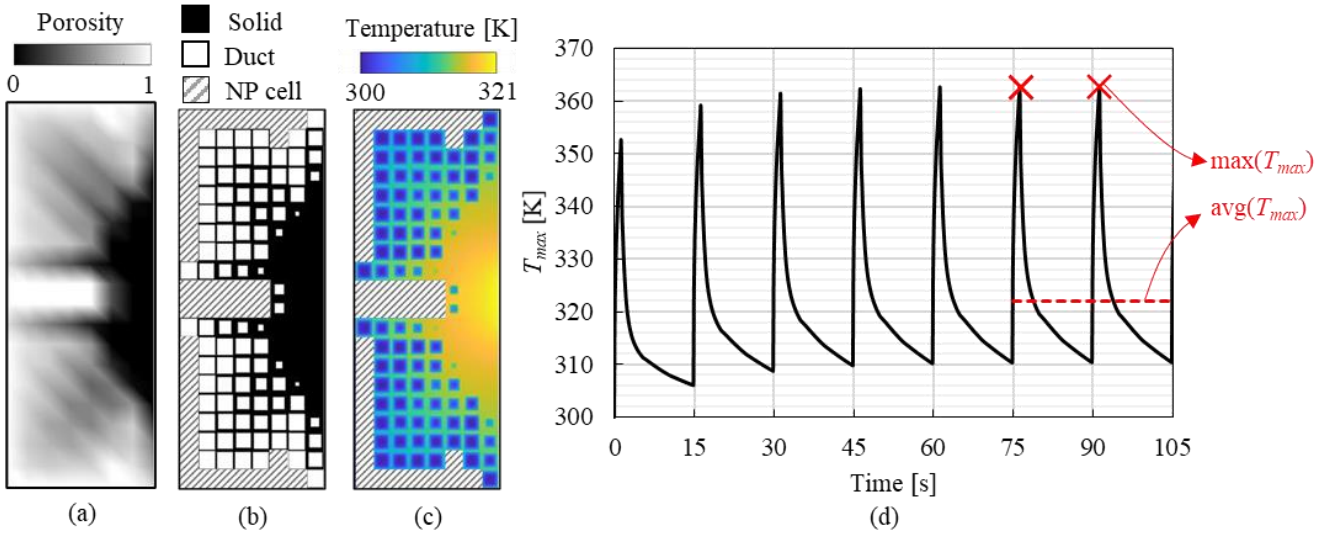

Fig. 3. Steady topology optimized heat sink with no solid wall thickness constraint imposed over the heater. For the optimized heat sink under a steady load of 10 W/cm^2: (a) grayscale representation of design domain based on the cell porosity; (b) physical heat sink design with black regions denoting solid (conduction pathways), white representing air ducts in the cell, and gray region representing non-participatory (NP) cells; and (c) temperature map. (d) Transient thermal response of the same heat sink under the pulsed periodic heat load in terms of maximum domain temperature with time.

to 0.625 mm). The domain has a depth Δz = 50 mm. The solid phase is assumed to be aluminum with a thermal conductivity of 130 W/m-K. A 10 × 50 mm^2 heat input is at the center of the right boundary wall, and the other walls are assumed adiabatic. A constant heat flux of 10 W/cm^2 is applied for the steady topology optimization. A fictitious pulsed periodic heat input is used to illustrate the transient performance characterization. The total period of the cycle is 15 s, with a pulse heat load of 100 W/cm^2 for the first 1.5 s, followed by 0 W/cm^2 for 13.5 s, such that the average is 10 W/cm^2. The solid wall thickness imposed over the heater, l_w, is increased in steps of 2.5 mm from 0 mm to 20 mm to manage the peak transient temperatures in the domain under the application of the pulsed periodic load. The air flows in a direction into the page through the ducts present in each cell. Air is assumed to enter the ducts at an inlet temperature of 300 K. A constant pressure drop of 100 Pa between the inlets and outlets of the ducts is considered for calculating flow velocities and mass flow rates. The low airflow rates at this pressure drop across the heat sink are representative of the conditions for a compact laptop as a point of reference only.

During optimization, sensitivity at each cell is calculated using SLP, and the porosities are updated based on the filtered sensitivities. For this study, a filtering radius of 3.75 mm was used to prevent any checkerboard pattern in the design. The cells are initialized at a uniform porosity, ε_i = 0.4, except when a solid wall is imposed at the heater, where a porosity of 0 is constrained. The performance of the optimized designs was confirmed to be insensitive to this initialization value. The mass constraint penalization factor α is held constant at a value of 1 in this study. The maximum solid mass fraction, M_{max}, is specified to be a constant at 0.7. This value was selected so that the designs were not highly constrained by weight, and the final value of solid mass fraction M for the optimized designs in this study was always found to be much lower than M_{max} for the given boundary and operating conditions. As an implementation check, when setting the M_{max} constraint to a lower value, it was observed that the optimizer did forego thermal performance to meet the stricter weight limit.

A. Steady optimization

A grayscale image of the cell porosity throughout the design domain, a physical representation of the optimized heat sink, and a temperature map depicting average cell temperature, T_s with fluid inlet temperature, $T_{f,in}$ in the duct are shown in Fig. 3a-c, respectively, for the case in which there was no additional wall thickness imposed over the heater. In the formulation, if the optimizer forces the duct size to approach the cell size, the effective thermal conductivity of the cell reduces drastically to a negligible value, leading to no heat being transferred to the air in that cell duct. Hence, cells with porosities greater than or equal to 0.9 are considered to be 'non-participatory,' and can be altogether removed from the heat sink; in practice, these regions could be blocked off with the inlet and outlet flow headers. Such non-participatory (NP) cells are shown with gray diagonal striping in Fig. 4b-c. A maximum temperature of ~321 K occurs in the domain at the heater for this steady heat load boundary condition, i.e., a temperature rise of ~21 K above the air inlet temperature. The optimizer creates a solid zone close to the heater to spread heat away from the source. The heat is then removed from the domain through convection at the solid-fluid interface in the ducts. It was generally observed that cells further away from the heater have larger air ducts and a smaller solid fraction, as there are lower heat fluxes that can be transferred easily to the air through convection.

B. Transient optimization

The transient response of the maximum temperature in the

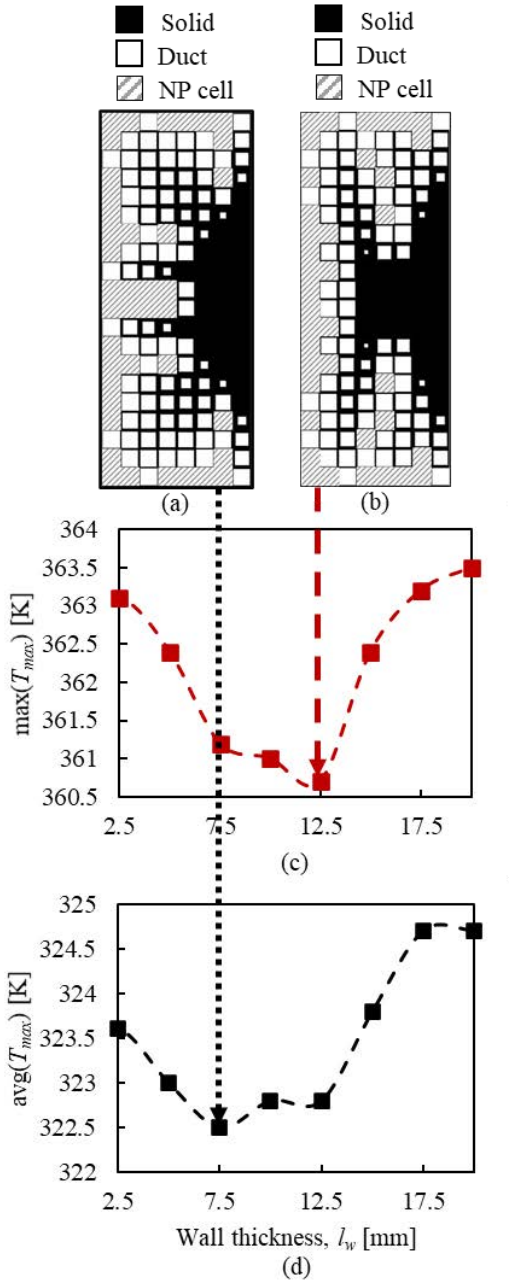

Fig. 4. Steady state topology optimized heat sink with wall thickness, l_w, equal to (a) 7.5 mm and (b) 12.5 mm. Transient performance of steady optimized heat sinks with increasing heater wall thickness in terms of the (c) peak transient maximum temperature, max(T_{max}), and (d) time-averaged maximum temperature, avg(T_{max}).

design domain, for the same topology optimized heat sink with no imposed heater wall thickness, is shown in Fig. 3d. The domain is initialized at the same temperature as the fluid inlet temperature of 300 K, and a pulsed periodic heat load is applied at the heater. During peak heat loading of 100 W/cm^2, the temperatures of the cells close to the heater rise rapidly, as observed by the sharp rise in the maximum domain temperature up to the peak in Fig. 3d. After peak loading for 1.5 s, no heat is supplied into the domain for the next 13.5 s; thus, the domain slowly cools down as thermal energy is conducted away from the source and dissipated by convection. This cycle of sharp temperature rise followed by slower cooling continues for every heat loading cycle until eventually the thermal response of the domain also becomes time-periodic.

For the heat sink design shown in Fig. 3, the thermal response becomes periodic after 75 s (5 cycles). After the domain achieves periodicity in thermal response, the transient performance is characterized per the max(T_{max}) and avg(T_{max}) metrics, which are marked in Fig. 3d using red crosses and a red dashed line, respectively. It was observed that time-averaged maximum temperature avg(T_{max}) relates directly to the maximum temperature of the domain under the steady heat load. For the heat sink design in Fig. 3, avg(T_{max}) is 322 K, and the maximum domain temperature under the steady heat load is 321 K. Hence, the use of steady topology optimization ensures optimal value for avg(T_{max}) when the heat sink design is characterized for transient performance.

The effects of imposing a solid wall of increased thickness l_w over the heater are shown in Fig. 4c-d, which respectively plot the peak and time-averaged transient maximum temperature in the domain versus the wall thickness. The addition of a wall thickness (to some extent) shows improved performance compared to the case without this constraint, owing to the added thermal capacitance as hypothesized above. While the magnitude of the improvement is modest for this particular case, a reduction of ~2–3 K, it importantly illustrates the existence of designs that are better performing for transient pulse loads than would otherwise be generated by a steady state topology optimizer without this subroutine. In particular, it was observed that a heat sink at one of the intermediate heater wall thickness of 12.5 mm gave the best-performing design in terms of the transient peak temperature, showing there is an optimal wall thickness for which the transient performance of the heat sink can be most improved. A lower wall thickness of 7.5 mm yields a design with the minimum time-averaged maximum temperature, showing the ability of the designer to weigh between max(T_{max}) and avg(T_{max}) within this range of wall thicknesses. A higher wall thickness than 12.5 mm attempts to reduce max(T_{max}) by further ensuring that the heat pulse is conducted away from the heater, but the occupation of a large portion of the domain by the wall takes away freedom from the optimizer to create ducts for convection, ultimately leading to a higher value of avg(T_{max}) and, in turn, a higher max(T_{max}).

IV. CONCLUSIONS

In this study, a steady topology optimization algorithm is formulated for the design of air-cooled heat sinks, with an intuition-based scheme to guide the optimizer toward improving the transient performance in response to heat pulses. A homogenization approach to topology optimization was used, which allows the specification of ducts of varying sizes within the domain to physically define the intermediate design variable porosities during iteration, unlike a traditional penalization approach. A variable heat transfer coefficient can thereby be calculated locally for each cell using correlations for flow inside a duct given the physical representation of partial porosities. Further, caloric resistance due to sensible heating of air is considered in the present formulation.

We demonstrate the use of this steady state topology optimization algorithm to reduce the peak temperature rise in the heat sink in response to a pulsed periodic heat load. Two metrics were used to characterize transient thermal performance, the transient peak maximum temperature in the domain, max(T_{max}), and the time-averaged maximum temperature, avg(T_{max}). It was observed that the steady-state heat sink performance directly corresponds with avg(T_{max}), and thus the use of steady topology optimization ensured optimal time-averaged temperature. However, to optimize for max(T_{max}), along with further reducing avg(T_{max}), a wall of increasing thickness is imposed over the heater area in the domain, and designs were generated for this constrained domain using steady topology optimization. It was observed that there exists an optimal added thickness at which the transient performance of the heat sink is most improved, either in terms of the peak or time-averaged maximum domain temperature. For air cooling of high-power devices that operate with a transient heat load, this combined topology optimization and intuition-based design approach would prove to be useful in managing the temperature swings in the system. The performance gains shown to be available herein also motivate further study of multi-physics, transient topology optimization approaches.

REFERENCES

[1] H.-S. P. Wong, K. Akarvardar, D. Antoniadis, J. Bokor, C. Hu, T.-J. King-Liu, S. Mitra, J. D. Plummer, S. Salahuddin, "A density metric for semiconductor technology," Proceedings of the IEEE, vol. 108, no. 4, pp. 478–482, 2020.

[2] J. L. Smoyer and P. M. Norris, "Brief historical perspective in thermal management and the shift toward management at the nanoscale," Heat Transfer Engineering, vol. 40, no. 3–4, pp. 269–282, 2019.

[3] M. Pecht, P. Lall, and E. B. Hakim, "The influence of temperature on integrated circuit failure mechanisms," Quality and Reliability Engineering International, vol. 8, no. 3, pp. 167–175, 1992.

[4] P. Rodgers, V. Eveloy, and M. G. Pecht, "Limits of air-cooling: status and challenges," in IEEE 21st Annual IEEE Symposium on Semiconductor Thermal Measurement and Management (SEMITHERM), 2005, pp. 116–124, 2005.

[5] Frank P. Incropera, *Liquid Cooling of Electronic Devices by Single-phase Convection*, Wiley, New York, 1999.

[6] I. Mudawar, "Two-phase microchannel heat sinks: theory, applications, and limitations," Journal of Electronic Packaging, vol. 133, no. 4, 2011.

[7] H. Y. Zhang, D. Pinjala, and P.-S. Teo, "Thermal management of high power dissipation electronic packages: from air cooling to liquid cooling," in Proceedings of the 5th Electronics Packaging Technology Conference (EPTC), pp. 620–625, 2003.

[8] R. C. Chu, R. E. Simons, M. J. Ellsworth, R. R. Schmidt, and V. Cozzolino, "Review of cooling technologies for computer products," IEEE Transactions on Device and Materials Reliability, vol. 4, no. 4, pp. 568–585, 2004.

[9] M. Wong, I. Owen, C. J. Sutcliffe, and A. Puri, “Convective heat transfer and pressure losses across novel heat sinks fabricated by Selective Laser Melting,” International Journal of Heat and Mass Transfer, vol. 52, no. 1, pp. 281–288, 2009.

[10] M. A. Arie, A. H. Shooshtari, and M. M. Ohadi, “Experimental characterization of an additively manufactured heat exchanger for dry cooling of power plants,” Applied Thermal Engineering, vol. 129, no. C, 2018.

[11] S. Ozguc, S. Pai, L. Pan, P. J. Geoghegan and J. A. Weibel, "Experimental demonstration of an additively manufactured vapor chamber heat spreader," in 18th IEEE Intersociety Conference on Thermal and Thermomechanical Phenomena in Electronic Systems (ITherm), 2019, pp. 416-422.

[12] H. A. Eschenauer and N. Olhoff, “Topology optimization of continuum structures: A review,” Applied Mechanics Reviews, vol. 54, no. 4, pp. 331–390, 2001.

[13] M. P. Bendsøe and O. Sigmund, *Topology Optimization*, Second Edition, Berlin, Heidelberg: Springer Berlin Heidelberg, 2004.

[14] E. M. Dede, S. N. Joshi, and F. Zhou, “Topology optimization, additive layer manufacturing, and experimental testing of an air-cooled heat sink,” Journal of Mechanical Design, vol. 137, no. 11, p. 111403, 2015.

[15] R. B. Haber and M. P. Bendsøe, “Problem formulation, solution procedures and geometric modeling: Key issues in variable-topology optimization,” in Proceedings of the 7th AIAA/USAF/NASA/ISSMO Symposium on Multidisciplinary Analysis and Optimization, pp. 1864–1873, 1998.

[16] S. Ozguc, L. Pan, and J. A. Weibel, “Topology optimization of microchannel heat sinks using a homogenization approach,” International Journal of Heat and Mass Transfer, vol. 169, p. 120896, 2021.

[17] H. P. de Bock, D. Huitink, P. Shamberger, J. S. Lundh, S. Choi, N. Niedbalski, L. Boteler, “A system to package perspective on transient thermal management of electronics,” Journal of Electronic Packaging, vol. 142, no. 4, 2020.

[18] J. Mathew and S. Krishnan, “A review on transient thermal management of electronic devices,” Journal of Electronic Packaging, vol. 144, no. 1, 2021.

[19] M. Pecht and Jie Gu, “Physics-of-failure-based prognostics for electronic products,” Transactions of the Institute of Measurement and Control, vol. 31, no. 3–4, pp. 309–322, 2009.

[20] S. Wu, Y. Zhang, and S. Liu, “Topology optimization for minimizing the maximum temperature of transient heat conduction structure,” Structural and Multidisciplinary Optimization, vol. 60, no. 1, pp. 69–82, 2019.

[21] J. Asmussen, J. Alexandersen, O. Sigmund, and C. S. Andreasen, “A ‘poor man’s’ approach to topology optimization of natural convection problems,” Structural and Multidisciplinary Optimization, vol. 59, no. 4, pp. 1105–1124, Apr. 2019.

[22] O. Sigmund, “Morphology-based black and white filters for topology optimization,” Structural and Multidisciplinary Optimization, vol. 33, no. 4, pp. 401–424, 2007.